SCIENCE CHINA
Information Sciences

• LETTER •

August 2025, Vol. 68, Iss. 8, 180511:1–180511:2
https://doi.org/10.1007/s11432-024-4515-1

Special Topic: Quantum Information

GHZ-W genuinely entangled subspace verification with adaptive local measurements

Congcong ZHENG[1,2,4], Ping XU[3], Kun WANG[3*] & Zaichen ZHANG[2,4,5*]

[1] *State Key Lab of Millimeter Waves, Southeast University, Nanjing 211189, China*
[2] *Frontiers Science Center for Mobile Information Communication and Security, Southeast University, Nanjing 210096, China*
[3] *College of Computer Science and Technology, National University of Defense Technology, Changsha 410073, China*
[4] *Purple Mountain Laboratories, Nanjing 211111, China*
[5] *National Mobile Communications Research Laboratory, Southeast University, Nanjing 210096, China*

Received 26 December 2024/Revised 1 April 2025/Accepted 3 July 2025/Published online 10 July 2025

Citation Zheng C C, Xu P, Wang K, et al. GHZ-W genuinely entangled subspace verification with adaptive local measurements. Sci China Inf Sci, 2025, 68(8): 180511, https://doi.org/10.1007/s11432-024-4515-1

Quantum entanglement is a fundamental aspect of quantum physics [1]. A key area of research in multipartite entanglement focuses on subspaces composed entirely of genuinely multipartite entangled states, known as the genuinely entangled subspace (GES) [2]. A notable example of a GES is the GHZ-W subspace, spanned by the GHZ and W states. The GHZ-W subspace has garnered significant attention due to its broader implications in multipartite entanglement theory. Notably, the three-qubit GHZ-W subspace serves as a universal resource for three-qubit entangled symmetric states. However, experimentally constructing three-qubit entangled symmetric resources remains challenging due to the pervasive influence of quantum noise. Consequently, accurately detecting the entanglement of the GHZ-W subspace has become a critical task in quantum information science. Recently, several approaches have been proposed to tackle this challenge, including subspace self-testing [2] and subspace verification [3].

We first review the framework of subspace verification. Let $\mathscr{D}(\mathcal{V})$ be the set of density operators acting on the target subspace $\mathcal{V}$ and Π be the projector onto $\mathcal{V}$. For a sequence of states $\sigma_1, \ldots, \sigma_N$, our task is to distinguish between the following two cases: (i) good: for all $i \in [N]$, $\mathrm{Tr}[\Pi\sigma_i] = 1$; (ii) bad: for all $i \in [N]$, $\mathrm{Tr}[\Pi\sigma_i] \leqslant 1-\epsilon$ for some fixed ϵ. To achieve this, assume that we have a set of POVM elements $\mathcal{M}$. For each state, we select a POVM element $M \in \mathcal{M}$ with probability $\mu(M)$ and perform the corresponding POVM with two results $\{M, \mathbb{1} - M\}$, where the M outputs "pass" and the $\mathbb{1} - M$ outputs "fail". The operator M is called a test operator and we require $\mathrm{Tr}[M\rho] = 1$ for all $\rho \in \mathscr{D}(\mathcal{V})$ and $M \in \mathcal{M}$. The sequence of states passes the verification procedure if all outcomes are "pass". Define the verification operator as $\Omega = \sum_{M\in\mathcal{M}} \mu(M)M$. If $\mathrm{Tr}[\Pi\sigma_i]$ is upper bounded by $1-\epsilon$, the probability of passing N tests is bounded by $(1-\nu(\Omega)\epsilon)^N$, where $\nu(\Omega) := 1 - \lambda_{\max}(\widehat{\Omega})$ is the spectral gap, $\widehat{\Omega} := (\mathbb{1} - \Pi)\Omega(\mathbb{1} - \Pi)$, and $\lambda_{\max}(X)$ denotes the maximum eigenvalue of X. To achieve a confidence level of $1-\delta$, the minimum required number of state copies is

$$N(\Omega) = \left\lceil \frac{1}{\ln(1-\nu(\Omega)\epsilon)^{-1}} \ln\frac{1}{\delta} \right\rceil \approx \left\lceil \frac{1}{\nu(\Omega)} \times \frac{1}{\epsilon} \ln\frac{1}{\delta} \right\rceil. \quad (1)$$

This equality provides a guide for the construction of efficient verification strategies by maximizing $\nu(\Omega)$. If there is no restriction on measurements, the globally optimal strategy is achieved by simply performing the projective measurement $\{\Pi, \mathbb{1} - \Pi\}$, and we have

$$N_G(\Pi) = \left\lceil \frac{1}{\epsilon} \ln\frac{1}{\delta} \right\rceil. \quad (2)$$

However, this strategy requires highly entangled measurements if the target subspace is genuinely entangled, which are experimentally challenging. In the following, we propose two efficient strategies to verify the subspace $\mathcal{V}_3 := \mathrm{span}\{|\mathrm{GHZ}\rangle, |\mathrm{W}\rangle\}$ with local measurements, where

$$|\mathrm{GHZ}\rangle := \frac{1}{\sqrt{2}}(|000\rangle + |111\rangle), \quad (3a)$$

$$|\mathrm{W}\rangle := \frac{1}{\sqrt{3}}(|001\rangle + |010\rangle + |100\rangle). \quad (3b)$$

We begin by constructing multiple test operators based on one-way adaptive measurements. Then, we propose two efficient verification strategies and analyze complexities.

Test operators. We randomly measure a qubit in the Pauli basis $P \in \{X, Z\}$. Each measurement yields one of two possible outcomes, "+" and "−". The remaining two qubits are projected into a two-qubit subspace spanned by two post-measurement states, called the post-measurement subspace. Subsequently, we apply the two-qubit subspace test operator. Therefore, the corresponding one-way adaptive test operators induced by P are given by

$$M_P = P^+ \otimes M_P^+ + P^- \otimes M_P^-. \quad (4)$$

* Corresponding author (email: nju.wangkun@gmail.com, zczhang@seu.edu.cn)

Concretely, for the post-measurement subspace induced by the Pauli Z measurement, the test operators are

$$M_Z^+ = \mathbb{1} - |11\rangle\langle 11|, \qquad M_Z^- = |00\rangle\langle 00| + |11\rangle\langle 11|. \tag{5}$$

The test operator induced by the Z measurement is

$$M_Z = |0\rangle\langle 0| \otimes M_Z^+ + |1\rangle\langle 1| \otimes M_Z^-. \tag{6}$$

Actually, this test operator can be implemented non-adaptively by performing the Z measurements on each qubit. Likewise, for the post-measurement subspace induced by the X measurement, the test operators are given by

$$M_X^+ = |x_+x_+\rangle\langle x_+x_+| + |\bar{x}_+\bar{x}_+\rangle\langle \bar{x}_+\bar{x}_+|, \tag{7}$$
$$M_X^- = \mathbb{1} - |x_-x'_-\rangle\langle x_-x'_-|, \tag{8}$$

where the states are defined as $|x_+\rangle = \cos\alpha|0\rangle + \sin\alpha|1\rangle$, $|\bar{x}_+\rangle = \sin\alpha|0\rangle - \cos\alpha|1\rangle$, $|x_-\rangle = (|0\rangle + \mathrm{e}^{\mathrm{i}\frac{\pi}{3}}|1\rangle)/\sqrt{2}$, $|x'_-\rangle = (|0\rangle + \mathrm{e}^{-\mathrm{i}\frac{\pi}{3}}|1\rangle)/\sqrt{2}$, and $\alpha = \arctan(\sqrt{5}-1)/2$. The resulting test operator induced by the X measurement is

$$M_X = |+\rangle\langle +| \otimes M_X^+ + |-\rangle\langle -| \otimes M_X^-. \tag{9}$$

An important observation from quantum state verification is that the local symmetry of the target can be exploited to create more test operators from current test operators [4]. Thus, we consider the following two local symmetries of $\mathcal{V}_3$.

(1) Qubit permutations:

$$V_\sigma := \sum_{i_1,i_2,i_3} |i_{\sigma^{-1}(1)} i_{\sigma^{-1}(2)} i_{\sigma^{-1}(3)}\rangle\langle i_1 i_2 i_3|, \tag{10}$$

where σ ranges over all elements of the symmetric group $\mathbb{S}_3$.

(2) Local unitaries: $U_1 := R_{2\pi/3}^{\otimes 3}$ and $U_2 := R_{4\pi/3}^{\otimes 3}$, where $R_\phi := |0\rangle\langle 0| + \mathrm{e}^{\mathrm{i}\phi}|1\rangle\langle 1|$.

Notice that M_Z is invariant under the above local symmetries, so we focus on M_X. First, for the qubit permutation symmetry, we define $M_{X,i}$ ($i = 1,2,3$) as a set of new test operators, where an X measurement is performed on the i-th qubit, followed by a two-qubit verification based on the measurement result. Then, for the local unitary symmetry, $U_j^\dagger M_{X,i} U_j$ ($j = 1,2$) are also valid one-way adaptive test operators. Physically, $U_j^\dagger M_{X,i} U_j$ corresponds to first applying the local rotation operator U_j to the quantum state, followed by the test operator $M_{X,i}$.

XZ strategy. Now, we propose a verification strategy using the 4 test operators constructed above, termed the XZ strategy. In each round, we select $P \in \{X, Z\}$ according to $\mu(P)$. If the Z measurement is chosen, we perform M_Z. Otherwise, we choose a qubit $i \in \{1,2,3\}$ uniformly at random to perform $M_{X,i}$. Mathematically, the verification operator is

$$\Omega_{XZ} = \mu(Z) M_Z + \frac{1}{3}\mu(X) \sum_{i=1}^{3} M_{X,i}. \tag{11}$$

We numerically analyze the performance of the verification operator Ω_{XZ} and show that $\max \nu(\Omega_{XZ}) \approx 0.262$ when $\mu(Z) \approx 0.424$. Therefore, to achieve a confidence level of $1-\delta$, we have

$$N(\Omega_{XZ}) \approx \left\lceil 3.817 \times \frac{1}{\epsilon} \ln \frac{1}{\delta} \right\rceil. \tag{12}$$

Rotation strategy. Then, we introduce the rotation strategy with the 10 test operators. In each round, we select $P \in \{X, Z\}$ according to a probability distribution $\mu(P)$. If the Z measurement is chosen, we perform M_Z. Otherwise, we apply U_1, U_2 or $\emptyset$ (no unitary at all) uniformly at random, followed by choosing one qubit uniformly at random to perform $M_{X,i}$. This can be written as

$$\widehat{M}_X := \frac{1}{3} \sum_{i=1}^{3} M'_{X,i}, \tag{13}$$

where $M'_{X,i} := \frac{1}{3}(M_{X,i} + U_1^\dagger M_{X,i} U_1 + U_2^\dagger M_{X,i} U_2)$. Therefore, the verification operator for this strategy is given by

$$\Omega_\mu := \mu(Z) M_Z + \mu(X) \widehat{M}_X. \tag{14}$$

The optimal probability distribution can be determined analytically, as shown in Proposition 1.

Proposition 1. The strategy operator defined in (14), achieves the largest spectral gap of 141/317 when $\mu^\star(X) = 240/317$.

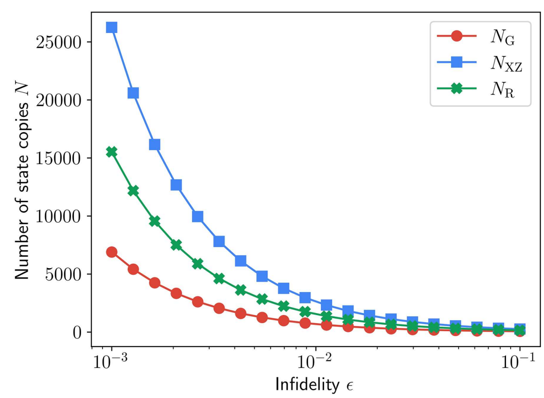

Figure 1 (Color online) Comparison of the total number of state copies required to verify the three-qubit GHZ-W subspace for different strategies with fixed $\delta = 0.001$. Here, N_G is given in (2), N_{XZ} is given in (12), and N_R is given in (15).

Therefore, to achieve a confidence level of $1-\delta$, we have

$$N(\Omega_{\mu^\star}) = \left\lceil \frac{317}{141} \times \frac{1}{\epsilon} \ln \frac{1}{\delta} \right\rceil \approx \left\lceil 2.248 \times \frac{1}{\epsilon} \ln \frac{1}{\delta} \right\rceil. \tag{15}$$

In Figure 1, we compare the efficiency of these strategies.

Acknowledgements This work was supported by National Key R&D Program of China (Grant No. 2022YFF0712800), National Natural Science Foundation of China (Grant No. 62471126), Jiangsu Key R&D Program Project (Grant No. BE2023011-2), SEU Innovation Capability Enhancement Plan for Doctoral Students (Grant No. CXJH_SEU 24083), and Fundamental Research Funds for the Central Universities (Grant No. 2242022k60001).

Supporting information The supporting information is available online at info.scichina.com and link.springer.com. The supporting materials are published as submitted, without typesetting or editing. The responsibility for scientific accuracy and content remains entirely with the authors.

References

1 Horodecki R, Horodecki P, Horodecki M, et al. Quantum entanglement. Rev Modern Phys, 2009, 81: 865–942
2 Baccari F, Augusiak R, Šupić I, et al. Device-independent certification of genuinely entangled subspaces. Phys Rev Lett, 2020, 125: 260507
3 Zheng C, Yu X, Zhang Z, et al. Efficient verification of stabilizer code subspaces with local measurements. 2024. ArXiv:2409.19699
4 Pallister S, Linden N, Montanaro A. Optimal verification of entangled states with local measurements. Phys Rev Lett, 2018, 120: 170502